The Astrophysical Journal, 657: L5–L8, 2007 March 1

SYSTEMATIC UNCERTAINTIES IN STELLAR MASS ESTIMATION FOR DISTINCT GALAXY POPULATIONS

Sheila J. Kannappan[1,2] and Eric Gawiser[1,3]

Received 2006 November 20; accepted 2007 January 19; published 2007 February 12

ABSTRACT

We show that different stellar mass estimation methods yield overall mass scales that disagree by factors up to ~2 for the $z = 0$ galaxy population and, more importantly, *relative* mass scales that sometimes disagree by factors $\gtrsim 3$ between distinct classes of galaxies (spiral/irregular types, classical E/S0s, and E/S0s whose colors reflect recent star formation). This comparison considers stellar mass estimates based on (1) two different calibrations of the correlation between *K*-band mass-to-light ratio and $B - R$ color and (2) detailed fitting of *UBRJHK* photometry and optical spectrophotometry using two different population synthesis models (Bruzual-Charlot and Maraston), with the same initial mass function in all cases. We also compare stellar+gas masses with dynamical masses. This analysis offers only weak arguments for preferring a particular stellar mass estimation method, given the plausibility of real variations in dynamical properties and dark matter content. These results help to calibrate the systematic uncertainties inherent in mass-based evolutionary studies of galaxies, including comparisons of low- and high-redshift galaxies.

Subject heading: galaxies: evolution

1. INTRODUCTION

The modern trend toward studying galaxy properties as a function of mass rather than luminosity has led to remarkable advances in our understanding of galaxy evolution, making the calibration of mass estimation techniques a high priority. Based on comparisons of dynamical and stellar mass ($M_{\rm dyn}$ and M_*) estimates, Drory et al. (2004) and Rettura et al. (2006) argue that multiband photometry alone can provide accurate M_* estimates that correlate well with $M_{\rm dyn}$. Even better, modeling of the correlation between optical colors and stellar mass-to-light ratios M_*/L suggests that factor of 2 accuracy in M_* may be achievable with just three filters, especially when using optical colors to infer an *I*- or *K*-band M_*/L (Bell & de Jong 2001; Portinari et al. 2004). However, recent work (Maraston 2005) cautions that M_* estimation may be more complicated than previously assumed, as young stellar populations may contribute substantially to not only optical but also near-infrared light, via thermally pulsing asymptotic giant branch (TP-AGB) stars. Using these models and those of Bruzual & Charlot (2003), van der Wel et al. (2006) find substantial inconsistencies between $M_{\rm dyn}$ and M_* estimates at low and high z that appear only when near-IR photometry is used.

To date, empirical examinations of these issues have relied on mixed data sets, making it hard to isolate systematics in M_* estimation from evolution between low- and high-redshift galaxies and/or effects of inhomogeneous data. Here we take advantage of the high-quality, uniform data available for the Nearby Field Galaxy Survey (NFGS; Jansen et al. 2000b), including photometry, spectrophotometry, and gas and stellar kinematics, to evaluate M_* estimation techniques. Our sample allows us to explore effects of stellar population age on M_* estimation at a single redshift, as it includes late-type galaxies, classical E/S0 galaxies that fall on the red color–M_* sequence, and galaxies with E/S0 morphologies that fall on the blue color–M_* sequence due to recent star formation ("blue-sequence E/S0s"; Kannappan et al. 2006, hereafter KGB).

[1] NSF Astronomy and Astrophysics Postdoctoral Fellow.

[2] Department of Astronomy, University of Texas at Austin, Austin, TX; sheila@astro.as.utexas.edu.

[3] Department of Astronomy, Yale University, New Haven, CT; gawiser@astro.yale.edu.

2. METHODS

The NFGS provides a broadly representative galaxy sample spanning a wide range of luminosities and morphologies. For M_* estimation, we analyze 141 NFGS galaxies with *UBRJHK* photometry and integrated (slit-scanned) optical spectrophotometry from Jansen et al. (2000a, 2000b) and the Two Micron All Sky Survey (2MASS) Extended Source Catalog (Jarrett et al. 2000); see KGB for sample selection details. Photometry and spectra are corrected for foreground extinction using Schlegel et al. (1998) and the Galactic extinction curve of O'Donnell (1994). We also check our results using *ugr* photometry for 92 of these galaxies, taken from the Sloan Digital Sky Survey (SDSS; Adelman-McCarthy et al. 2006), adopting SDSS "model" magnitudes corrected for cataloged foreground extinction. We do not apply internal extinction corrections to the data used for mass determination (although corrections based on the method of Tully et al. 1998 are used incidentally for defining the red and blue sequences, with no effect on our mass error budget; see KGB). However, dust is either included in our modeling or, in the case of color-M_*/L relations, neglected following standard practice. We add 0.1 mag in quadrature to the catalogued internal magnitude uncertainties for all passbands to account for systematic uncertainties in foreground extinction corrections, automated 2MASS photometry (see Bell et al. 2003, hereafter B03), and relative photometric zero points. For the spectra, we add relative flux calibration uncertainties (typically 6%, but up to 9% outside 4000–6800 Å; R. Jansen 2002, private communication) in quadrature to the formal uncertainties.

Our "reference" M_* values are computed by fitting the photometry and spectra to a discrete grid of stellar population synthesis models from Bruzual & Charlot (2003) scaled to a "diet Salpeter" initial mass function (IMF) as used by B03. We combine two simple stellar populations (SSPs) in varying mass fractions (100% : 0%, 90% : 10%, 80% : 20%, etc.), where we have normalized each SSP to $M_* = 1\ M_\odot$. Each individual SSP has one of eight ages (0.025, 0.1, 0.29, 0.64, 1, 2.5, 5, and 11 Gyr) and three metallicities (0.4, 1, and 2.5 $Z_\odot$), and each combination of SSPs has one of 11 dust optical depths ($\tau_{V,\,\rm gas} = 0$, 0.12, 0.24, …, 1.2). We derive model photometry by convolving NFGS (standard Johnson-Cousins), SDSS, and 2MASS filter profiles with Bruzual-Charlot model spec-

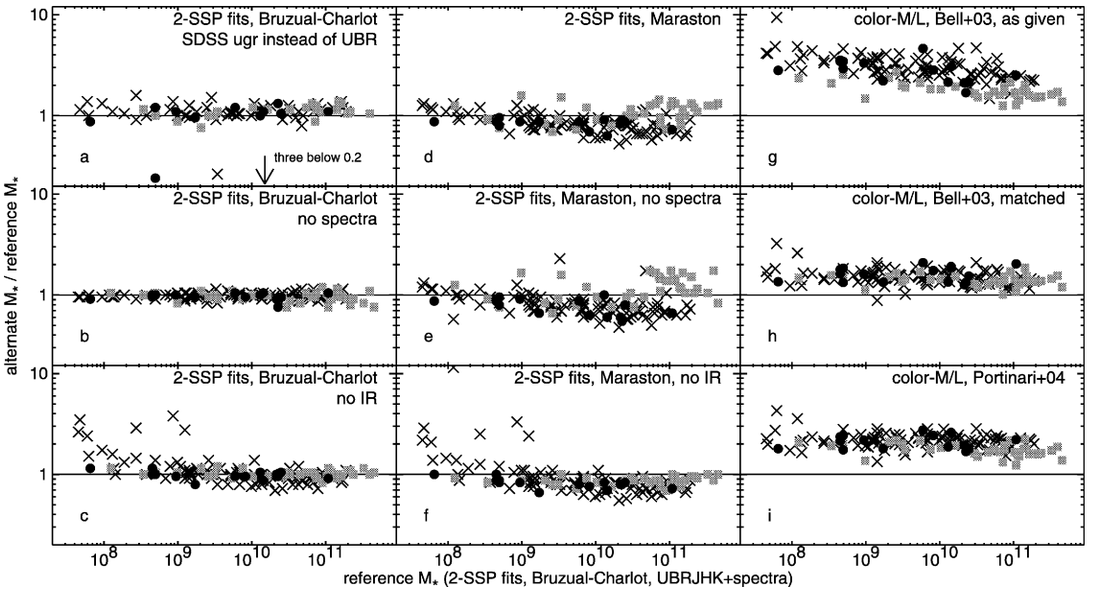

FIG. 1.—Comparison of M_* estimates obtained by various methods, with symbols coded to show spiral/irregular types (*crosses*), red-sequence E/S0s (*gray squares*), and blue-sequence E/S0s (*black dots*). Each panel shows the ratios between M_*'s computed by an alternate method, as noted, and our reference M_*'s computed by fitting Bruzual-Charlot models to *UBRJHK*+spectrophotometry, with ratios plotted as a function of reference M_*.

tra and adding attenuation using a Calzetti (2001) law. The code scales each model to the observed photometry in $L_\odot$ units, yielding the estimated M_* for that model, then computes likelihoods $\propto e^{-\chi^2_{\rm overall}/2}$ for the entire grid of models. In a first pass, we fit only the photometry, redshifting the models to match the individual galaxy spectroscopic redshifts and comparing with redshift-zero models to determine *k*-corrections. In a second pass, the likelihood-weighted average *k*-corrections are applied to the input photometry, and the code fits both the photometry and the deredshifted spectra to a fixed set of models in the rest frame. We mask emission lines, limit the spectral range to 3800–7000 Å, and convolve the model spectra to the 6 Å resolution of the NFGS spectra. As the spectra lack absolute flux calibration, their scale factors are allowed to vary freely. The likelihood of each model is the product of the likelihoods inferred from the photometry and the spectra, so the χ^2 terms sum in the exponent and can be weighted to set the relative influence of the spectra and photometry. We adopt $\chi^2_{\rm overall} = \max(\chi^2_{\rm phot}, n_{\rm dof}) + \chi^2_{\rm spec\text{-}raw}/1000 + \chi^2_{\rm spec\text{-}norm}/1000$, where the latter two terms are contributions from fits to the raw and continuum-normalized spectra and $n_{\rm dof}$ is the number of degrees of freedom in $\chi^2_{\rm phot}$, normally five when fitting six filters (losing one to the scale-factor determination). Once the photometric data are reasonably well fit ($\chi^2_{\rm phot} \leq n_{\rm dof}$), the likelihoods are affected only by the spectra. Otherwise, the likelihoods are equally influenced by the reduced χ^2 values of the spectra and photometry, because the ratio of the number of data points is ~500 (where the strong covariance between $\chi^2_{\rm spec\text{-}raw}$ and $\chi^2_{\rm spec\text{-}norm}$ justifies treating them as a joint $\chi^2_{\rm spec}$ term). Following Bundy et al. (2005) we adopt the median of the likelihood distribution binned over $\log M_*$ rather than the best fit to determine the final M_*, and we estimate uncertainties from the 68% confidence interval in $\log M_*$ (binning in 0.02 dex intervals).

M_* estimates based on the $B-R$ versus M_*/L_K relation are derived from the calibrations of B03 and Portinari et al. (2004, hereafter P04). The B03 calibration is based on a global linear fit to M_*/L_K versus synthetic $B-R$ for a large sample of galaxies with *ugrizK* data, where each galaxy is fitted with PEGASE population synthesis models (Fioc & Rocca-Volmerange 1997) to find the best-fit metallicity and exponential star formation history (SFH), which may be decaying, constant, or rising. The P04 calibration is predicted from chemophotometric models of galactic disks, which include TP-AGB stars. We use the Salpeter IMF calibration from P04, multiplying the resulting masses by 0.7 to match the diet Salpeter IMF scale of B03. Technically, P04 limit their calibration to $B-R = 0.95$–1.45, and our use of the relation sometimes extends outside this range. Factor of 2 uncertainties are predicted for color-based mass estimation, primarily due to variations in SFH but also due to the neglect of internal reddening and extinction (expected to vary mainly along the $B-R$ vs. M_*/L_K relation; see Bell & de Jong 2001). Because color M_*/L relations do not provide a self-consistent way to compute *k*-corrections, we *k*-correct the input magnitudes using our standard method described above.

When comparing M_* and $M_{\rm dyn}$, we apply more restrictive sample selection criteria. After rejecting galaxies flagged as morphologically peculiar by Kannappan et al. (2002, hereafter KFF), we define two subsamples for which mass estimates should be robust: (1) 38 spiral/irregular galaxies with both H I data from the HyperLeda homogenized H I catalog (Paturel et al. 2003) and optical emission-line rotation curves passing the quality criteria of KFF, with the latter also having asymmetry <10% and extent >1.3 times the *B*-band half-light radius r_e^B (Kannappan & Barton 2004); and (2) 26 E/S0 galaxies with optical (Mg-triplet region) stellar velocity dispersions in the NFGS database (Kannappan & Fabricant 2001; S. J. Kannappan et al. 2007, in preparation), initially measured within $r_e^B/4$ using the Fourier-space fitting code of van der Marel & Franx (1993) and rescaled to the *R*-band half-light radius r_e^R using equation (1) of Cappellari et al. (2006). We require the rescaled dispersion to satisfy $\sigma_{r_e^R} > 120$ km s^{-1} to ensure negligible rotation corrections (see, e.g., KGB, Fig. 9).

For late types, gas masses are computed from the H I line flux with a helium-mass correction factor of 1.4 and a type- and mass-dependent molecular-gas correction factor of 1.06–1.4 (based on Casoli et al. 1998). We adopt an uncertainty of 50% in the total

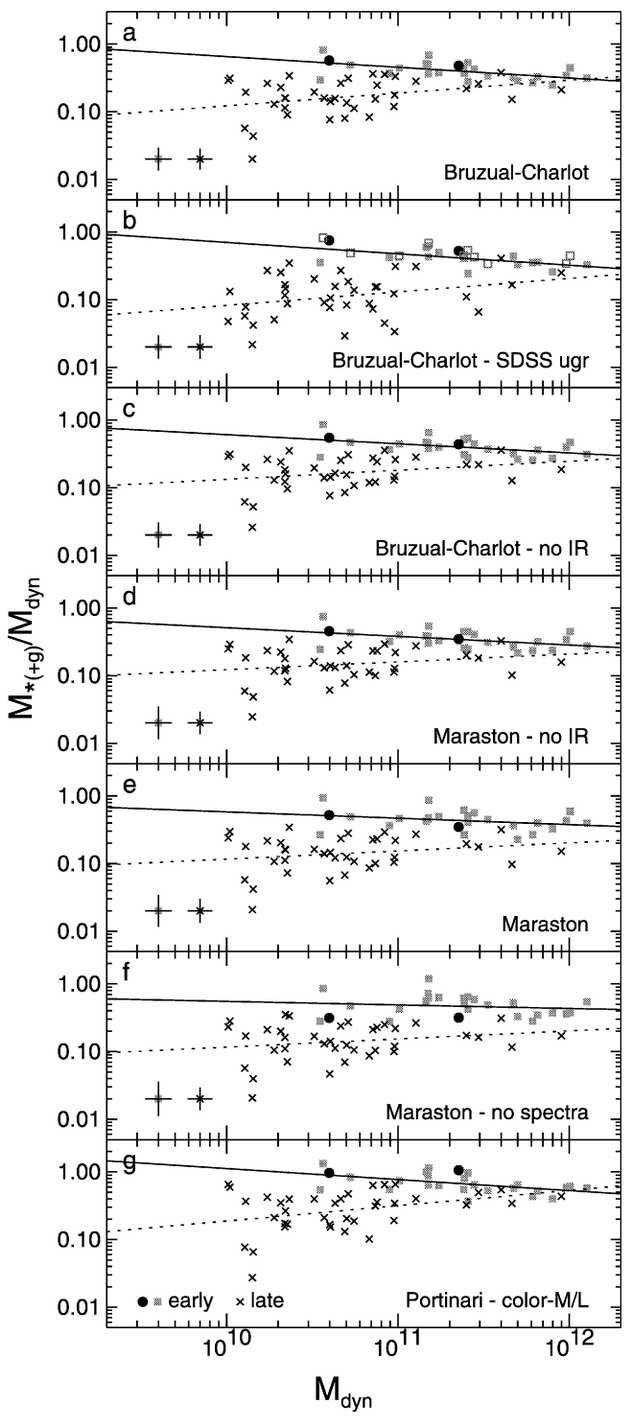

FIG. 2.—Comparison of $M_{*(+g)}$ (gas-mass corrected for late types only, § 2) and M_{dyn} for various methods of M_* estimation. Symbols are as in Fig. 1, with the addition of an open square symbol in panel *b* to mark E/S0s from panel *a* for which SDSS *ugr* data are not available. Least-squares fits and typical error bars are shown for early and late types, with blue-sequence E/S0s included with red-sequence E/S0s.

gas mass. For the E/S0s, which are all massive given our cut in $\sigma_{r_e^R}$, we assume gas masses are negligible (the largest measured gas-to-stellar mass ratio in this subsample is $\lesssim$15%).

Dynamical masses are computed for the E/S0 subsample using $M_{dyn} = 5r_e^R\sigma^2_{r_e^R}$, as recommended by Cappellari et al. (2006). We add 5% in quadrature to the uncertainties in r_e^R for profile extrapolation errors, and 5% and 7%, respectively, to the uncertainties in $\sigma_{r_e^R}$ for template mismatch and aperture rescaling errors. For the spiral/irregular subsample we use $M_{dyn} = 2.5r_e^R V^2_{rot}$, assuming V_{rot} scales like $\sqrt{2}\sigma$ (e.g., Burstein et al. 1997). Here V_{rot} is 0.5 times the inclination-corrected $W^i_{V_{pmm}}$ line width parameter of KFF.

We assume $H_0 = 70$ km s^{-1} Mpc^{-1} and $d = cz/H_0$. Note that our error bars do not include distance errors because distances are largely irrelevant to comparisons between mass estimates.

3. RESULTS

Various M_* estimation methods are compared in Figure 1, with the ratio between the alternate and reference M_*'s plotted as a function of reference M_* in each panel. Figure 2 compares $M_{*(+g)}$ estimates against M_{dyn} in the same format, where the notation $M_{*(+g)}$ indicates a gas mass correction for late types (§ 2). We stress that differences between methods do not imply that one or the other is correct, and differences relative to M_{dyn} must be interpreted carefully, given the potential for real variation in dark matter content or structural properties.

Figures 1*a*–1*c* and 2*a*–2*c* test the robustness of our reference M_*'s against substitution of *ugr* for *UBR*, omission of the spectra from the fits, and exclusion of the near-IR *JHK* data. Replacing *UBR* with *ugr*, a slight offset appears in Figure 1*a*. NFGS photometry appears more reliable: Figure 2*b* demonstrates that $M_{*(+g)}$ estimates based on SDSS photometry yield greater scatter relative to M_{dyn} for late-type galaxies, and inspection of the fits reveals that SDSS data have a fairly high rate of catastrophic errors relative to 2MASS and NFGS data, perhaps due to systematic errors in defining galaxy apertures or profiles. Note that the apparent improvement in scatter for E/S0 galaxies in Figure 2*b* is probably fortuitous: the open squares mark galaxies from Figure 2*a* that do not have SDSS data, showing that they tend to be the galaxies with the largest scatter. M_*'s obtained with and without spectra are closely consistent (Fig. 1*b*) and compare similarly with dynamical mass (not shown). Taking advantage of this result, we have verified that our reference M_*'s are robust to using a finer resolution in mass ratio between the two SSPs: 100% : 0%, 98% : 2%, 96% : 4%, etc., where for computational efficiency only the photometry is fitted. Finally, omission of near-IR data (Fig. 1*c*) produces generally consistent results, with a few outliers. The outliers are all late-type galaxies with fairly low surface brightness, whose 2MASS magnitudes may be underestimated. Alternatively, in such bursty systems, M_*/L may be overestimated without the IR data to anchor the fits. These systems do not show large shifts from Figure 2*a* to 2*c* because their $M_{*(+g)}$ is gas-dominated.

Substituting Maraston (2005) models for Bruzual-Charlot models, stronger differences emerge (Figs. 1*d*–1*f* and 2*d*–2*f*). Figure 1*d* shows a factor of 2 difference in the relative M_* scales of high-mass red-sequence E/S0s compared to both blue-sequence E/S0s and late-type galaxies. With spectra omitted (Fig. 1*e*), this difference grows to a factor of 3, whereas with near-IR *JHK* data omitted (Fig. 1*f*), it disappears entirely, although a small overall scale difference remains (with Maraston models yielding $\lesssim$1.3 times lower M_*). Excluding near-IR data, $M_{*(+g)}$ estimates based on Bruzual-Charlot and Maraston models compare nearly identically to M_{dyn} (Figs. 2*c*–2*d*). The differences when near-IR data are included come almost entirely

from the Maraston models and cause shifts relative to $M_{\rm dyn}$ in Figures 2*e*–2*f*. However, these shifts are within the uncertainties and might be physical: in a hierarchical scenario, late-type galaxies may have both more dark matter and more scatter in dark matter content than early-type galaxies. Also, blue-sequence E/S0s may have basic structural differences from red-sequence E/S0s that lead to overestimated $M_{\rm dyn}$, if their σ and/or r-values are elevated due to incomplete postmerger evolution or disk-building processes (KGB).

Figures 1*g*–1*i* and 2*g* examine M_* estimates based on color-M_*/L relations taken from B03 and P04. Using the B03 relation as given, we find strong disagreement compared to our reference M_*'s in both overall mass scale and relative scales between different galaxy classes, by factors $\gtrsim$3. However, inspection of the data from which the B03 relation was determined (their Fig. 20) reveals that their linear fit is skewed by a two-component distribution, consisting of a dominant linear locus and a cloud of outliers with blue colors and high M_*/L. These outliers may be analogous to the outliers we find in Figures 1*c* and 1*f* or may reflect low metallicities (B03). In any case, the overall trends can be harmonized if we refit the color-M_*/L relation of B03 using only the primary linear locus. Figure 1*h* demonstrates good agreement with only a small overall scale difference when we adopt the modified relation $\log(M_*/L_K) = -0.616 + 0.34(B-R)$ for $(B-R) > 1.2$ and $\log(M_*/L_K) = -0.808 + 0.5(B-R)$ for $(B-R) < 1.2$, fitted by eye to their Figure 20. These formulae include a factor of 1.2 to convert between the M_* scales of the PEGASE and Bruzual-Charlot models; this offset is noted by B03 when comparing their fit to earlier predictions from Bell & de Jong (2001) and can be estimated from their Figure 20. In addition to adopting a modified color-M_*/L relation, Figure 1*h* adjusts the color-based M_*'s for the influence of dust and starbursts. B03 estimate that dust and starbursts, if modeled, would decrease their M_* estimates by ~15% and ~10%, respectively, so we reduce M_*'s for galaxies with detected Hα by 15% and M_*'s for all galaxies except massive E/S0s ($M_* > 10^{11}\ M_\odot$) by a separate 10%. With this matched-B03 calibration, we find good agreement between the two color-based M_* estimation methods (Figs. 1*h*–1*i*), with overall scales ~1.5–1.8 times higher than our reference M_*'s, possibly due to differences in assumed SFHs and/or photometric zero points. There may be a slight tendency for the P04 calibration to give higher M_* to younger galaxies, which reduces the offset between E/S0s and late-type galaxies in comparison to $M_{\rm dyn}$ (Fig. 2*g*). This apparent improvement in the match between $M_{*(+g)}$ and $M_{\rm dyn}$ should be taken with a grain of salt, as it reflects the loss of information on why galaxies are blue or red (age, dust, metallicity).

In summary, our results demonstrate systematic uncertainties in M_* estimation corresponding to factors up to ~2 overall and $\gtrsim$3 between distinct galaxy classes, even using our modified B03 calibration and matched IMFs. Outliers affect the original color-M_*/L_K calibration of B03 and also emerge when we compare results from stellar population modeling with and without IR data (note both B03 and this work rely on 2MASS). More generally, M_* estimates are highly sensitive to IR and spectral information when using Maraston models, especially for red- and blue-sequence E/S0s. An Occam's razor argument might justify preferring Bruzual-Charlot models, which yield consistent results with or without spectra or IR data. However, we are unable to find a strong physical argument for preferring a particular set of models based on comparisons with $M_{\rm dyn}$, and we caution that agreement between $M_{*(+g)}$ and $M_{\rm dyn}$ is not by itself proof of better M_* estimation, given evidence for variations in dark matter content, dynamical state, and age/dust/metallicity. We conclude that mass-based evolutionary studies of galaxies should explicitly consider the potential effects of systematic errors in M_*, particularly when analyzing young and old galaxies together across galaxy classes or between low and high z.

We thank A. Baker, D. Christlein, K. Gebhardt, R. Jansen, I. Labbé, D. Mar, K. Williams, and M. Wolf for helpful discussions. S. J. K. and E. G. were supported by NSF Astronomy and Astrophysics Postdoctoral Fellowships under awards AST 04-01547 and 02-01667, respectively. This research used the HyperLeda H I catalog (Vizier Catalog VII/238) and data from 2MASS, a joint project of the University of Massachusetts and IPAC/Caltech, funded by NASA and the NSF. It also used data from the Sloan Digital Sky Survey (see full acknowledgement at http://www.sdss.org/collaboration/credits.html).

REFERENCES

Adelman-McCarthy, J. K., et al. 2006, ApJS, 162, 38
Bell, E. F., & de Jong, R. S. 2001, ApJ, 550, 212
Bell, E. F., McIntosh, D. H., Katz, N., & Weinberg, M. D. 2003, ApJS, 149, 289 (B03)
Bruzual, G., & Charlot, S. 2003, MNRAS, 344, 1000
Bundy, K., Ellis, R. S., & Conselice, C. J. 2005, ApJ, 625, 621
Burstein, D., Bender, R., Faber, S., & Nolthenius, R. 1997, AJ, 114, 1365
Calzetti, D. 2001, PASP, 113, 1449
Cappellari, M., et al. 2006, MNRAS, 366, 1126
Casoli, F., et al. 1998, A&A, 331, 451
Drory, N., Bender, R., & Hopp, U. 2004, ApJ, 616, L103
Fioc, M., & Rocca-Volmerange, B. 1997, A&A, 326, 950
Jansen, R. A., Fabricant, D., Franx, M., & Caldwell, N. 2000a, ApJS, 126, 331
Jansen, R. A., Franx, M., Fabricant, D., & Caldwell, N. 2000b, ApJS, 126, 271
Jarrett, T. H., Chester, T., Cutri, R., Schneider, S., Skrutskie, M., & Huchra, J. P. 2000, AJ, 119, 2498
Kannappan, S. J., & Barton, E. J. 2004, AJ, 127, 2694
Kannappan, S. J., & Fabricant, D. G. 2001, AJ, 121, 140
Kannappan, S. J., Fabricant, D. G., & Franx, M. 2002, AJ, 123, 2358 (KFF)
Kannappan, S. J., Guie, J. M., & Baker, A. J. 2006, AJ, submitted (KGB)
Maraston, C. 2005, MNRAS, 362, 799
O'Donnell, J. E. 1994, ApJ, 422, 158
Paturel, G., Theureau, G., Bottinelli, L., Gouguenheim, L., Coudreau-Durand, N., Hallet, N., & Petit, C. 2003, A&A, 412, 57
Portinari, L., Sommer-Larsen, J., & Tantalo, R. 2004, MNRAS, 347, 691 (P04)
Rettura, A., et al. 2006, A&A, 458, 717
Schlegel, D. J., Finkbeiner, D. P., & Davis, M. 1998, ApJ, 500, 525
Tully, R. B., Pierce, M. J., Huang, J., Saunders, W., Verheijen, M. A. W., & Witchalls, P. L. 1998, AJ, 115, 2264
van der Marel, R. P., & Franx, M. 1993, ApJ, 407, 525
van der Wel, A., Franx, M., Wuyts, S., van Dokkum, P. G., Huang, J., Rix, H.-W., & Illingworth, G. D. 2006, ApJ, 652, 97